Disorder-Free Localization

A. Smith,[1,*] J. Knolle,[1] D. L. Kovrizhin,[2,3] and R. Moessner[4]
[1]T.C.M. Group, Cavendish Laboratory, J. J. Thomson Avenue, Cambridge CB3 0HE, United Kingdom
[2]Rudolf Peierls Centre for Theoretical Physics, 1 Keble Road, Oxford OX1 3NP, United Kingdom
[3]NRC Kurchatov Institute, 1 Kurchatov Square, 123182 Moscow, Russia
[4]Max Planck Institute for the Physics of Complex Systems, Nöthnitzer Straße 38, 01187 Dresden, Germany
(Received 21 February 2017; published 27 June 2017)

The venerable phenomena of Anderson localization, along with the much more recent many-body localization, both depend crucially on the presence of disorder. The latter enters either in the form of quenched disorder in the parameters of the Hamiltonian, or through a special choice of a disordered initial state. Here, we present a model with localization arising in a very simple, completely translationally invariant quantum model, with only local interactions between spins and fermions. By identifying an extensive set of conserved quantities, we show that the system generates purely dynamically its own disorder, which gives rise to localization of fermionic degrees of freedom. Our work gives an answer to a decades old question whether quenched disorder is a necessary condition for localization. It also offers new insights into the physics of many-body localization, lattice gauge theories, and quantum disentangled liquids.

DOI: 10.1103/PhysRevLett.118.266601

The study of localization phenomena—pioneered in Anderson's seminal work on the absence of diffusion in certain random lattices [1]—is receiving redoubled attention in the context of the physics of interacting systems showing many-body localization [2–4]. While in these systems the presence of quenched disorder plays a central role, suggestions for interaction-induced localization in disorder-free systems appeared early in the context of solid helium [5]. However, all of these are limited to settings having inhomogeneous initial states [6,7]. Whether quenched disorder is a general precondition for localization has remained an open question. Here, we provide an explicit example to demonstrate that a disorder-free system can generate its own randomness dynamically, which leads to localization in one of its subsystems. Our model is exactly soluble, thanks to an extensive number of conserved quantities, which we identify, allowing access to the physics of the long-time limit. The model can be extended while preserving its solubility, in particular towards investigations of disorder-free localization in higher dimensions.

Localization phenomena are often diagnosed, in experiment and simulation, via the dynamical response to a global quantum quench. The underlying idea is to examine if a system thermalizes, thereby losing memory of the initial state, or whether this memory persists in the long-time limit [6–9]. Some of the simple initial states used in these diagnostics exhibit density modulations, e.g., in the form of a periodic density-wave pattern, or a density imbalance, with two halves of the system separated by a "domain wall." The latter setup was exploited in the experimental identification of the many-body localization (MBL) transition [10]. In this experiment a complete domain-wall melting was observed in the ergodic phase, while the density imbalance remained in the localized phase at long times, showing exponential tails set by the localization length [11]. Another useful localization diagnostic, which does not require inhomogeneous initial states, is based on examining deviations from linearity in the light-cone spreading of correlations after a quantum quench [12,13].

In translationally invariant systems, initial state inhomogeneity has been a precondition for the emergence of localization. For instance, in models containing a mixture of interacting heavy and light particles [6,7], the heavy particles play a role of quasistatic disorder for the light particles. However, these models show only transient subdiffusive behavior, which ultimately gives way to ergodicity at long times [6,14]. They were dubbed quasi-MBL. Related attempts concern localization in translationally invariant quantum versions of classical glassy models [15], whose behavior, so far, cannot be differentiated from quasi-MBL, due to limitations on system sizes available in numerical simulations. Our work may also provide a new perspective on quantum disentangled liquids [16–18], which are characterized by the lack of equilibration in one or more of the components of the liquid. Beyond this, only the construction of single-particle hopping problems with entirely flat dispersions, so that the group velocities of any wave packet vanish, has succeeded in stopping particles from moving [19,20].

The model, which we present here, exhibits localization of purely dynamical origin. This localization is induced by a quantum quench, and we use the above-mentioned standard diagnostics to examine its nature. We stress that our model is entirely disorder free, namely, both the

 © 2017 American Physical Society

Hamiltonian, and—crucially—initial states do not require any quenched disorder. On the technical side we can analyze the nature of dynamically generated randomness, thanks to an extensive set of conserved quantities. We show that time evolution after a quantum quench is described by a dual Hamiltonian with binary disorder. This allows us to develop an efficient numerical algorithm to access system sizes far beyond the localization length, allowing us to conclude that the phenomenology detailed below is representative of the thermodynamic limit.

The Letter is structured in the following way. First, we introduce the model and define the quench protocols we consider. Second, we identify the conserved charges and how they are associated with the dynamically generated randomness. Third, we present our results for the fermionic and the spin subsystems of our model. For the fermionic subsystem we can extract a length scale, which we compare with the relevant single-particle localization length. Finally, we close with a discussion where we make connections to related models and progress currently being made in the field. An outline of the numerical methods we use is referred to the Supplemental Material [21].

Model.—We study a 1D lattice model of spinless fermions $\hat{f}_i$ that are coupled via spins 1/2, $\hat{\sigma}_{i,i+1}$, positioned on the bonds. The model is described by the Hamiltonian (Fig. 1)

$$\hat{H} = -J\sum_{\langle ij\rangle}\hat{\sigma}^z_{i,j}\hat{f}^\dagger_i\hat{f}_j - h\sum_i\hat{\sigma}^x_{i-1,i}\hat{\sigma}^x_{i,i+1}. \tag{1}$$

Here, J and h denote the fermion tunneling strength and Ising coupling, respectively. In the following we discuss dynamics induced by the Hamiltonian (1) on initial states with all bond spins aligned with the z axis, and the fermions prepared in a Slater determinant. We consider three distinct examples of the latter: (i) domain wall $|1\ldots111000\ldots0\rangle$; (ii) density wave $|\ldots10101\ldots\rangle$, and (iii) the translationally invariant ground state of the Hamiltonian (1) at $h = 0$.

Dynamically generated randomness.—The model possesses an extensive set of conserved quantities $\{q_j\}$ identified through the duality mapping, known from the Ising model [25,26]. This holds for arbitrary initial fermion states. In the subspace fixed by a particular set of $\{q_j\} = \pm1$ the Hamiltonian (1) assumes a simple noninteracting form

$$\hat{H}_{\{q_j\}} = -J\sum_{\langle ij\rangle}\hat{c}^\dagger_i\hat{c}_j + 2h\sum_j q_j(\hat{c}^\dagger_j\hat{c}_j - 1/2), \tag{2}$$

a tight-binding model with a binary potential given by the charge sector $\{q_j\}$. Note that, despite the simplicity of Eq. (2), the dynamics of the physical system is highly nontrivial, not least on account of the nonlinear transformation between degrees of freedom of the physical Hamiltonian (1) and dual Hamiltonian (2).

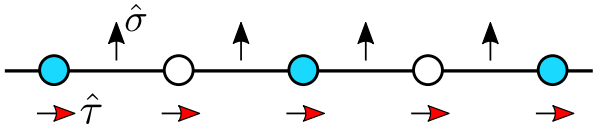

FIG. 1. Schematic picture of the model. The signs of nearest-neighbor hopping for spinless fermions (blue circles) are determined by the z components of the σ spins (black arrows) living on the bonds. Dual τ spins (red arrows, see the Supplemental Material [21]) are shown in the configuration corresponding to the σ spins.

The identification of the set of conserved quantities $\{q_j\}$ and the derivation of Eq. (2) proceed by a duality mapping [25,26] from bond spins σ to site spins τ,

$$\hat{\tau}^z_j = \hat{\sigma}^x_{j-1,j}\hat{\sigma}^x_{j,j+1}, \qquad \hat{\sigma}^z_{j,j+1} = \hat{\tau}^x_j\hat{\tau}^x_{j+1}. \tag{3}$$

We consider a system of N sites with open boundary conditions, see Fig. 1. Periodic boundary conditions introduce only a few technical differences, such as the global constraint on spins, which is automatically satisfied by our choice of initial spin states (for more details see, e.g., Refs. [12,27]). In terms of the dual spins, the Hamiltonian assumes the following form:

$$\hat{H} = -J\sum_{\langle ij\rangle}\hat{\tau}^x_i\hat{\tau}^x_j\hat{f}^\dagger_i\hat{f}_j - h\sum_i\hat{\tau}^z_i. \tag{4}$$

Here, N mutually commuting conserved charges are given by $\hat{q}_j \equiv \hat{\tau}^z_j(-1)^{\hat{n}_j}$ with $\hat{n}_j = \hat{f}^\dagger_j\hat{f}_j$. The charges also commute with the Hamiltonian $\hat{H}$, but change sign under the action of operators $\hat{\tau}^x_j$, and $\hat{f}^{(\dagger)}_j$. In terms of new fermion operators $\hat{c}_j = \hat{\tau}^x_j\hat{f}_j$, which commute with the charges, one arrives at the Hamiltonian (2).

We restrict initial states at $t = 0$ to tensor products of fermion and spin states $|0\rangle = |S\rangle \otimes |\psi\rangle$. The z-polarized initial state of bond spins $|S\rangle = |\uparrow\uparrow\uparrow\cdots\rangle_\sigma$ implies a sum over all 2^N charge configurations $\{q_i\} = \pm1$,

$$|0\rangle = \frac{1}{2^{N/2}}\sum_{\{q_i\}=\pm1}|q_1, q_2, \ldots, q_N\rangle \otimes |\psi\rangle, \tag{5}$$

which leads to correlators averaged over a binary potential. This particular initial spin state ensures that the tensor product of spin and fermion states $|S\rangle \otimes |\psi\rangle_f$ translates into a tensor product of charge configurations and fermion states $|Q\rangle \otimes |\psi\rangle_c$ after the transformation from Eq. (1) to Eq. (2), which would not generally be the case. However, we find that this is not crucial for the observed phenomenology, see the Supplemental Material [21] for more details. Note that states akin to Eq. (5) were suggested in Ref. [28] for quantum simulations of disordered systems.

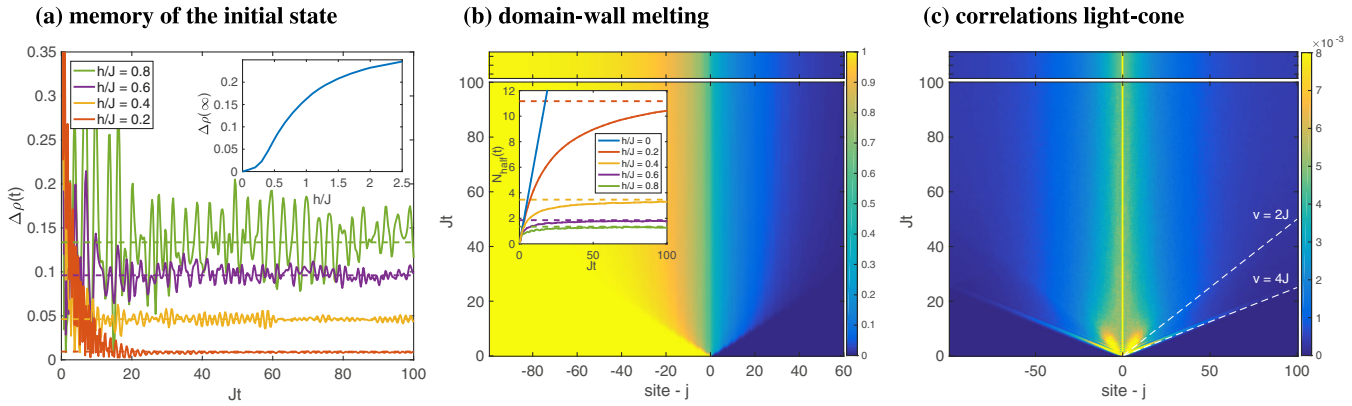

FIG. 2. Time evolution of the fermion subsystem. (a) $\Delta\rho(t)$, after a quench from a density wave initial state, for a range of values h/J, with the dashed lines showing a long-time limit. Inset: long time limit of $\Delta\rho$ as a function of h/J. (b) Fermion density for a domain-wall initial state at $h/J = 0.3$. Inset: integrated fermion number in the right half of the chain as a function of time. (c) Absolute value of the connected density-density correlator $\langle 0|\hat{n}_l(t)\hat{n}_{l+j}(t)|0\rangle_c$ for a density-wave initial state at $h/J = 0.2$. The dashed lines correspond to two light-cone velocities. The upper panels in (b) and (c) show the long-time limit $Jt = 10^9$. All figures are computed for systems with $N = 200$ sites.

In our model this state appears naturally from a translationally invariant initial state.

Results.—The identification of the conserved charges, and the form of the dual Hamiltonian (2), allow us to evaluate correlators, which we will use to demonstrate disorder-free dynamical localization. The results presented below were obtained for systems with up to $N = 200$ sites, see the Supplemental Material [21].

Fermionic subsystem.—First, we consider the fermionic subsystem, see Fig. 2. For a density-wave initial state

$$\Delta\rho(t) = \frac{1}{N}\sum_j |\langle 0|\hat{n}_j(t) - \hat{n}_{j+1}(t)|0\rangle| \qquad (6)$$

measures the average staggered fermion density. In an ergodic phase, $\Delta\rho(t)$ vanishes at long times. In our model, it instead shows saturation to a finite asymptotic value $\Delta\rho(\infty)$, Fig. 2(a), which grows monotonically with h/J (inset). This demonstrates the persistence of memory of the initial state.

Similarly, for the domain-wall initial state [10,11], with a maximal density imbalance between two halves of the lattice, Fig. 2(b), an initial spreading of fermions eventually halts, and the number of particles emitted from the filled to the empty half of the system after the quench, N_{half}, (inset) remains finite. The long-time spatial density distribution shows exponential tails. The decay length is simply proportional to the single-particle localization length [29], as in Ref. [11], see Fig. 3, with a proportionality constant of approximately 2.

Next, we diagnose localization via connected density-density correlators $\langle 0|\hat{n}_j(t)\hat{n}_k(t)|0\rangle_c$. In the absence of dynamical disorder, $h = 0$, we observe the light-cone spreading of a free-fermion model [12], whose envelop is set by the velocity corresponding to the Lieb-Robinson bound $v_{\text{LR}} = 4J$, twice the maximum fermion group velocity. This is in contrast with quenches for $h \neq 0$ [Fig. 2(c)]. For a density-wave initial state at short times, the linear spreading of correlators, bounded by v_{LR}, and accompanied by a second signal at $v_{\text{LR}}/2$, is eventually suppressed at long times. In this limit the correlators assume a stationary form [13], decaying with the same exponent as the density imbalance, Fig. 3. We emphasise that we find a similar localization behavior for a translationally invariant Fermi-sea initial state, some results for which are shown in the Supplemental Material [21].

This above ensemble of results provides unambiguous evidence of localization of the fermionic subsystem in a model without quenched disorder. This is our first central result.

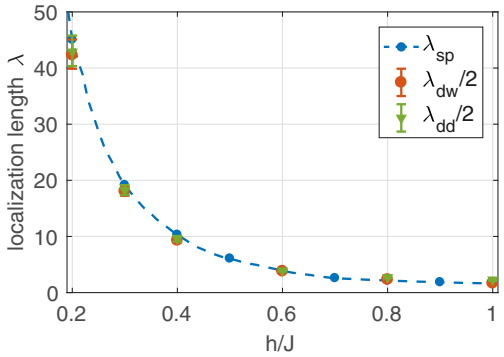

FIG. 3. The localization length. Length scales determined from the tails $\sim\exp(-j/\lambda)$ in the long-time limit of the density imbalance (λ_{dw}, circles), the density-density correlators (λ_{dd}, triangles), and the single-particle localization length (λ_{sp}) [29]. The error bars are given by 2.5 standard deviations of the numerical exponential fit. For $h/J = 0.2$, 0.3 we used $N = 400$, with $N = 200$ for all others.

Spin subsystem.—Let us now turn to the discussion of results for the spin subsystem. The expectation value of the z component of the bond spin, Fig. 4(a), decays to zero at long times for all $h \neq 0$. Furthermore, for the explored range of parameters h/J, we find that this decay is asymptotically a power law. The remarkable qualitative agreement between the exact result for $N = 20$ and the disorder averaged result for $N = 200$ suggests that the spin dynamics is dominated by regions of finite size, presumably of the order of the fermion localization length. Intriguingly, we find persistent spin fluctuations accompanying the power-law decay.

The equal-time spin correlator on two bonds, Fig. 4(b), exhibits an initial linear light cone. As with the fermion correlators, the extent of the ballistic regime is determined by the localization length. As for the spin average, we find a decay of all spatial correlations to zero in the long-time limit, indicating equilibration of the spin subsystem.

Discussion.—We have observed dynamical localization after a completely translationally invariant quantum quench. The fermionic subsystem retains memory of the initial state, whereas the spin subsystem eventually equilibrates. In our model of fermions coupled to dynamical spins, the requisite randomness is generated dynamically. The main technical advance of our work is the identification of an extensive set of conserved $\mathbb{Z}_2$ charges such that the time evolution can be described by a noninteracting Hamiltonian with effective binary disorder, allowing numerical computations on large systems.

Despite the close relation of our model to the heavy-light mixtures studied in the context of quasi-MBL [6,7], we identify several key differences. First, the only limit where true nonergodicity is known in these models is an infinite mass "heavy" species, whereas the corresponding limit for us ($h \to 0$) amounts to free fermions. Otherwise the dynamics of the heavy species generally leads to the eventual return of ergodicity [6,14], whereas we observe complete localization for all $h \neq 0$. We can also vary the parameter h/J freely; thus, there is no meaningful distinction in our model in terms of heavy or light particles: the two subsystems are instead characterized by equilibration or lack thereof. This is similar to the distinction between the components of quantum disentangled liquids [16–18]. Interestingly, the model of Eq. (2) is also related to the Falikov-Kimbell model of Ref. [30], which shows a rich phase diagram at finite temperature.

The tunability of h/J may be important for experimental realizations, as varying h/J can change the localization length, e.g., in the range 0.2–1 from 100 down to almost a single lattice spacing. This could enable quantum simulations even on the currently available relatively small systems [31].

Moreover, our setup itself is remarkably simple: the Hamiltonian contains just nearest-neighbor exchange and hopping terms, while the initial state can be chosen as a simple, entirely unentangled product state of spins and

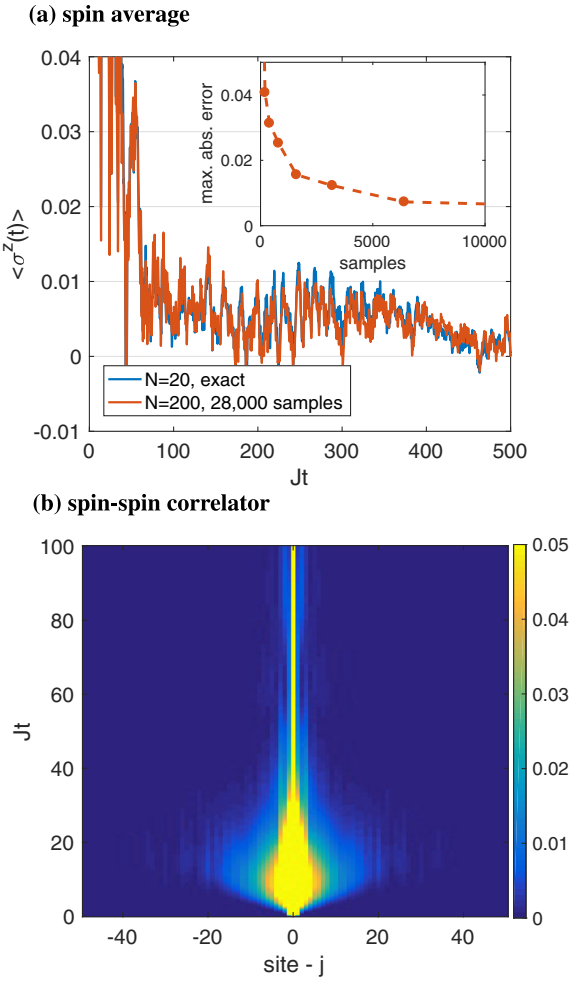

FIG. 4. Time evolution of the spin subsystem. (a) The spin average $\langle \hat{\sigma}^z(t) \rangle$ of the bond spin at $h/J = 1$ after a quench from an initial half-filled Fermi-sea state, comparing the exact result for $N = 20$ with the disorder averaged result for $N = 200$. Inset: maximum absolute error of disorder sampling, compared with the exact summation over all spin configurations, as a function of the number of samples for $N = 15$, $h/J = 1$. (b) Absolute value of the connected spin correlator $\langle \hat{\sigma}^z_l(t) \hat{\sigma}^z_{l+j}(t) \rangle_c$ for $h/J = 0.3$, $N = 100$.

fermions, thereby removing obstacles related to preparing complex many-body states. This should enable our proposal to take maximal advantage from recent progress in quantum simulations of lattice gauge theories [32].

Indeed, there are numerous connections to gauge theories appearing in other contexts. Our model can be thought of as a fermionic matter field minimally coupled to a dynamical gauge field with a somewhat unusual Hamiltonian. It is less constrained, but related to $\mathbb{Z}_2$-slave-spin representations of the Hubbard model, and of lattice gauge theories [33–35]. Crucially, our model allows for straightforward generalizations, in particular to higher dimensions, yielding, e.g., Kitaev's toric code model coupled to fermionic matter. This holds the promise of studying, in a broad range of settings, the novel localization phenomena uncovered in this work.

We are grateful to J. T. Chalker, F. H. L. Essler, C. Castelnovo, and A. Nahum for enlightening discussions. A. S. would like to acknowledge the EPSRC for studentship funding under Grant No. EP/M508007/1. J. K. is supported by the Marie Curie Programme under EC Grant Agreements No. 703697. The work of D. L. K. was supported by EPSRC Grant No. EP/M007928/1. R. M. was in part supported by the DFG under Grant No. SFB 1143.

*as2457@cam.ac.uk

[1] P. W. Anderson, Phys. Rev. **109**, 1492 (1958).
[2] D. Basko, I. Aleiner, and B. Altshuler, Ann. Phys. (Amsterdam) **321**, 1126 (2006).
[3] R. Vasseur and J. E. Moore, J. Stat. Mech.: Theory Exp. (**2016**) P064010.
[4] R. Nandkishore and D. A. Huse, Annu. Rev. Condens. Matter Phys. **6**, 15 (2015).
[5] Y. Kagan and L. A. Maksimov, Sov. Phys. JETP **60**, 201 (1984).
[6] N. Y. Yao, C. R. Laumann, J. I. Cirac, M. D. Lukin, and J. E. Moore, Phys. Rev. Lett. **117**, 240601 (2016).
[7] M. Schiulaz, A. Silva, and M. Müller, Phys. Rev. B **91**, 184202 (2015).
[8] T. Enss, F. Andraschko, and J. Sirker, Phys. Rev. B **95**, 045121 (2017).
[9] M. Schreiber, S. S. Hodgman, S. Bordia, H. P. Lüschen, M. H. Fischer, R. Vosk, E. Altman, U. Schneider, and I. Bloch, Science **349**, 842 (2015).
[10] J.-Y. Choi, S. Hild, J. Zeiher, P. Schauss, A. Rubio-Abadal, T. Yefsah, V. Khemani, D. A. Huse, I. Bloch, and C. Gross, Science **352**, 1547 (2016).
[11] J. Hauschild, F. Heidrich-Meisner, and F. Pollmann, Phys. Rev. B **94**, 161109 (2016).
[12] F. H. L. Essler and M. Fagotti, J. Stat. Mech.: Theory Exp. (**2016**) P064002.
[13] M. Žnidarič, T. Prosen, and P. Prelovšek, Phys. Rev. B **77**, 064426 (2008).
[14] Z. Papić, E. M. Stoudenmire, and D. A. Abanin, Ann. Phys. (Amsterdam) **362**, 714 (2015).
[15] M. van Horssen, E. Levi, and J. P. Garrahan, Phys. Rev. B **92**, 100305 (2015).
[16] T. Grover and M. P. A. Fisher, J. Stat. Mech.: Theory Exp. (**2014**) P10010.
[17] T. Veness, F. H. L. Essler, and M. P. A. Fisher, arXiv: 1611.02075.
[18] J. R. Garrison, R. V. Mishmash, and M. P. A Fisher, Phys. Rev. B **95**, 054204 (2017).
[19] D. H. Dunlap and V. M. Kenkre, Phys. Rev. B **34**, 3625 (1986).
[20] J. Vidal, R. Mosseri, and B. Doucot, Phys. Rev. Lett. **81**, 5888 (1998).
[21] See Supplemental Material at http://link.aps.org/supplemental/10.1103/PhysRevLett.118.266601 for details, which includes Refs. [22–24].
[22] D. L. Kovrizhin and J. T. Chalker, Phys. Rev. B **81**, 155318 (2010).
[23] D. J. Thouless, J. Phys. C **5**, 77 (1972).
[24] A. Weiße, G. Wellein, A. Alvermann, and H. Fehske, Rev. Mod. Phys. **78**, 275 (2006).
[25] H. A. Kramers and G. H. Wannier, Phys. Rev. **60**, 252 (1941).
[26] E. Fradkin and L. Susskind, Phys. Rev. D **17**, 2637 (1978).
[27] N. Iorgov, V. Shadura, and Y. Tykhyy, J. Stat. Mech.: Theory Exp. (**2011**) P02028.
[28] B. Paredes, F. Verstraete, and J. I. Cirac, Phys. Rev. Lett. **95**, 140501 (2005).
[29] B. Kramer and A. MacKinnon, Rep. Prog. Phys. **56**, 1469 (1993).
[30] A. E. Antipov, Y. Javanmard, P. Ribeiro, and S. Kirchner, Phys. Rev. Lett. **117**, 146601 (2016).
[31] J. Zhang, P. W. Hess, A. Kyprianidis, P. Becker, A. Lee, J. Smith, G. Pagano, I. D. Potirniche, A. C. Potter, A. Vishwanath, N. Y. Yao, and C. Monroe, Nature (London) **543**, 217 (2017).
[32] E. A. Martinez, C. A. Muschik, P. Schindler, D. Nigg, A. Erhard, M. Heyl, P. Hauke, M. Dalmonte, T. Monz, P. Zoller, and R. Blatt, Nature (London) **534**, 516 (2016).
[33] A. Rüegg, S. D. Huber, and M. Sigrist, Phys. Rev. B **81**, 155118 (2010).
[34] R. Žitko and M. Fabrizio, Phys. Rev. B **91**, 245130 (2015).
[35] S. Gazit, M. Randeria, and A. Vishwanath, Nat. Phys. **13**, 484 (2017).